An RNA Interference/Adeno-Associated Virus Vector–Based Combinatorial Gene Therapy Approach Against Hepatitis E Virus

Cindy Zhang,[1,2,4] Andrew Freistaedter,[2] Carolin Schmelas,[1] Manuel Gunkel,[3] Viet Loan Dao Thi ,[2,4*] and Dirk Grimm[1,4,5*]

Hepatitis E virus (HEV) is a major public health problem with limited therapeutic options. Here, we engineered adeno-associated viral vectors of serotype 6 (AAV6) to express short hairpin RNAs (shRNAs) against HEV transcripts with the prospect of down-regulating HEV replication *in vivo*. We designed 20 different shRNAs, targeting the genome of the HEV genotype 3 (GT3) Kernow-C1 p6 strain, for delivery upon AAV6 transduction. Using an original selectable HEV GT3 reporter replicon, we identified three shRNAs that efficiently down-regulated HEV replication. We further confirmed their inhibitory potency with full-length HEV infection. Seventy-two hours following transduction, HEV replication in both systems decreased by up to 95%. The three most potent inhibitory shRNAs identified were directed against the methyltransferase domain, the junction region between the open reading frames (ORFs), and the 3′ end of ORF2. Targeting all three regions by multiplexing the shRNAs further enhanced their inhibitory potency over a prolonged period of up to 21 days following transduction. *Conclusion:* Combining RNA interference and AAV vector–based gene therapy has great potential for suppressing HEV replication. Our strategy to target the viral RNA with multiplexed shRNAs should help to counteract viral escape through mutations. Considering the widely documented safety of AAV vector–based gene therapies, our approach is, in principle, amenable to clinical translation. (*Hepatology Communications* 2022;6:878-888).

Hepatitis E virus (HEV) is a nonenveloped, positive-strand RNA virus that is a major causative agent of acute fulminant hepatitis.[1] The 7.2-kb HEV genome encodes three open reading frames (ORFs) 1-3 (reviewed in Oechslin et al.[2]): ORF1 encodes the nonstructural proteins responsible for virus replication, ORF2 the capsid protein, and ORF3 a small phosphoprotein that mediates progeny virus secretion (Fig. 1A).

HEV is classified in its own *Hepeviridae* family[5] and is able to infect a wide range of hosts. Four major genotypes (GT 1-4) infect humans, which belong to the *Orthohepevirus A* genus.[5] GT1 and GT2 are transmitted fecal-orally and restricted to human infection, whereas GT3 and GT4 can be transmitted zoonotically (reviewed in Kamar et al.[1]) or through blood transfusions.[6] Recently, GT7[7] and a distantly related *Orthohepevirus C* GT1 rat HEV were also reported to infect humans.[8]

Abbreviations: AAV, adeno-associated virus; GFP, green fluorescent protein; GLuc, Gaussia luciferase; GT, genotype; HDV, hepatitis D virus; HEV, hepatitis E virus; HEV3 Rep/GLuc2ANeo, HEV GT3 replicon harboring neomycin phosphotransferase selection, 2A self-cleaving peptide sequence, and Gaussia luciferase reporter gene; HLC, hepatocyte-like cell; iPSC, induced pluripotent stem cell; ISLB, intrinsic stem-loop base; Met, methyltransferase; MOI, multiplicity of infection; ORF, open reading frame; RBV, ribavirin; RNAi, RNA interference; PCR, polymerase chain reaction; shCtrl, nontargeting shRNA control; shISLB, shRNA targeting the base of an intrinsic stem-loop in ORF2; shMet, shRNA targeting methyltransferase; shORF2, shRNA targeting the 3′end of ORF2; shRNA, short hairpin RNA; siRNA, small interfering RNA; trish scrbl Ctrl, triple scrambled shRNA control.

Received June 15, 2021; accepted October 10, 2021.

Additional Supporting Information may be found at onlinelibrary.wiley.com/doi/10.1002/hep4.1842/suppinfo.

**These authors contributed equally to this work.*

Supported by Deutsches Zentrum für Infektionsforschung, Deutsche Forschungsgemeinschaft (240245660 and 272983813), Chica and Heinz Schaller Foundation, and German Network for Bioinformatics Infrastructure (031A537C).

HEV infections are usually asymptomatic and self-limiting.[1] Yet, a high mortality has been observed in pregnant women infected with GT1 and 2 (reviewed in Pérez-Gracia et al.[9]). The zoonotic viruses, GT3 and GT4, can progress to chronic infection in immunocompromised patients and lead to progressive liver injury. In patients with chronic HEV, extrahepatic manifestations affecting peripheral nerves, kidney, and pancreas were reported (reviewed in Horvatits and Pischke[10]). Current therapies are based on off-label pegylated interferon-α and ribavirin (RBV).[11] However, resistance to the treatment and treatment failure have been reported.[12] We recently showed that sofosbuvir can inhibit HEV replication *in vitro* and proposed it as an add-on therapy to RBV.[13] Although sofosbuvir monotherapy reduced HEV-RNA levels in a small patient cohort, it failed to eradicate the virus.[14] Altogether, efficient and direct-acting therapies against HEV are still needed.

RNA interference (RNAi) is a sequence-specific process primarily used in mammals as a regulatory mechanism to control gene activity. It has also evolved as a potent natural defense mechanism against viral infections in other organisms, such as plants and invertebrates (reviewed in Schuster et al.[15]). RNAi relies on the delivery of small RNA molecules that are complementary to the target sequence. A convenient approach to produce these small RNA triggers is to use DNA-encoded short hairpin RNAs (shRNAs), which can be efficiently expressed by RNA polymerase III promoters. Once processed by the endogenous cellular machinery into small interfering RNAs (siRNAs), they contribute to the formation of the RNA-induced silencing complex (RISC). After removal of the nonbinding passenger strand, the functional RISC cleaves a fully complementary target sequence upon binding.

Notably, RNAi can be harnessed as a tool to control gene expression in genetic and infectious diseases, as validated in a variety of preclinical studies and culminating in multiple Food and Drug Administration (FDA)–approved drugs.[16-18] Most relevant in the context of the present study, RNAi has been repurposed to treat chronic viral infections, such as those with human immunodeficiency virus,[19] hepatitis B,[20] and/or hepatitis C virus.[21] In principle, because HEV is an RNA virus, it could be targeted by RNAi.

Despite the promise and potential of exogenously induced RNAi to control viral infections, data on its

View this article online at wileyonlinelibrary.com.
DOI 10.1002/hep4.1842

Potential conflict of interest: Dr. Grimm is co-founder and Chief Scientific Officer of AaviGen GmbH.

ARTICLE INFORMATION:

From the [1]Department of Infectious Diseases/Virology, Medical Faculty, Heidelberg University, Cluster of Excellence CellNetworks, BioQuant, Center for Integrative Infectious Diseases Research, Heidelberg, Germany; [2]Schaller Research group at Department of Infectious Diseases/Virology, Medical Faculty, Heidelberg University, Center for Integrative Infectious Diseases Research, Heidelberg, Germany; [3]High-Content Analysis of the Cell and Advanced Biological Screening Facility, BioQuant, Heidelberg University, Heidelberg, Germany; [4]German Center for Infection Research, Heidelberg, Germany; [5]German Center for Cardiovascular Research, Heidelberg, Germany.

ADDRESS CORRESPONDENCE AND REPRINT REQUESTS TO:

Viet Loan Dao Thi
Center for Integrative Infectious Diseases Research
University Hospital Heidelberg
Im Neuenheimer Feld 344
69120 Heidelberg, Germany
E-mail: VietLoan.DaoThi@med.uni-heidelberg.de
Tel.: +49 (0) 6221 563 56 43
or

Dirk Grimm
University of Heidelberg
BioQuant BQ0030
Im Neuenheimer Feld 267
69120 Heidelberg, Germany
E-mail: Dirk.Grimm@bioquant.uni-heidelberg.de
Tel.: +49 (0) 6221 545 1331

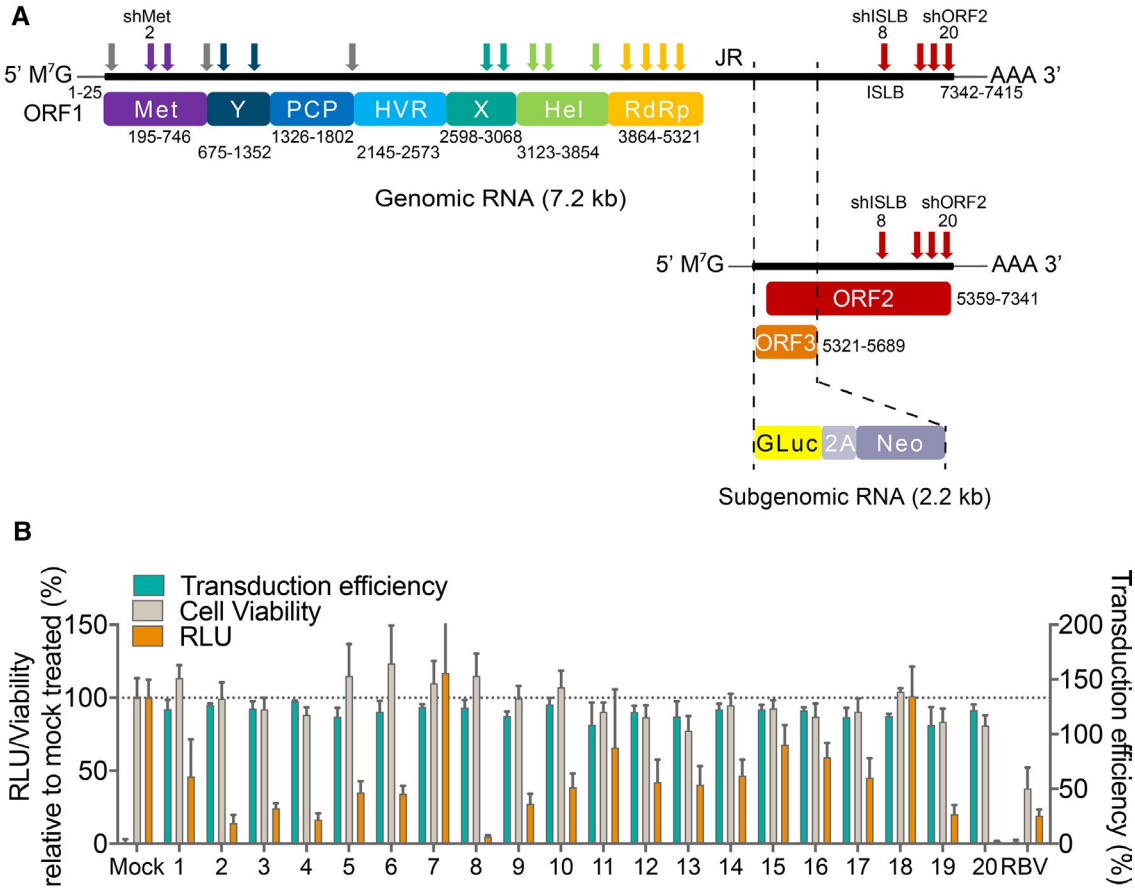

FIG. 1. Design and screening of shRNAs directed against the HEV genome using selectable reporter replicon. (A) Schematic depiction of the HEV GT3 selectable reporter replicon with targets of the 20 designed shRNAs (depicted as arrows), including domains in open reading frame 1 (ORF1) such as the methyltransferase (Met), the Y domain, the putative papain-cysteine like protease (PCP), the X domain, RNA helicase (Hel), and RNA-dependent RNA polymerase (RdRp), as well as domains in ORF2 such as the base of an intrinsic stem-loop area and the 3′ end of ORF2. Arrow colors show the target domain of the shRNAs. Gray-colored arrows represent shRNAs targeting sequences in between ORF domains, for which exact borders have not been defined yet.[3] Nucleotide positions refer to domain borders adapted from van Tong et al.[4] for HEV GT3 Kernow-C1 p6. (B) Screen of shRNA candidates on HEV3 Rep/GLuc2ANeo cells. Cells were transduced with 10 μL of AAV6-shRNA crude lysates or treated with 100 μM RBV as positive control. Medium was changed every 24 hours and GLuc secretion (relative light units, RLU), transduction efficiency (GFP %), and cell viability relative to mock-transduced cells were analyzed 72 hours following transduction. Results represent the mean of n = 6 ± SD. Abbreviations: HVR, hypervariable region; JR, junction region; M7G, 7-methylguanosine; shISLB, shRNA targeting base of intrinsic stem loop; shMet, shRNA targeting methyltransferase; and shORF2, shRNA targeting 3′ end of ORF2.

specific use as an anti-HEV modality are surprisingly scarce. Kumar et al. showed that HEV GT1 replicon replication can be inhibited by shRNAs *in vitro*.[22] *In vivo*, shRNAs conferred protection against HEV GT4 infection of piglets.[23] However, in this former work, the shRNAs were expressed from intravenously injected plasmid DNA, which is not readily translatable into humans, and it suffers from limited efficiency and specificity of shRNA delivery. Here, we screened a panel of shRNA for their potency in down-regulating the HEV GT3 Kernow-C1 p6 strain. To maximize clinical translatability, we used adeno-associated viruses (AAVs) for shRNA delivery, which are safe and promising vectors for therapeutic gene transfer in humans (reviewed in Borel et al.[24] and Zhan et al.[25]).

Materials and Methods

PLASMIDS AND CELLS

Plasmids encoding the HEV GT3 Kernow-C1 p6 strain (GenBank accession No: JQ679013) and S10-3 cells were a kind gift from Suzanne U. Emerson (National Institutes of Health, Bethesda, MD). S10-3 and HEK-293T cells were cultured in Dulbecco's modified Eagle medium (Gibco, Carlsbad, CA), supplemented with 10% fetal bovine serum (FBS; Merck, Darmstadt, Germany) and 1% penicillin-streptomycin (Gibco). Human induced pluripotent stem cells (iPSCs) were differentiated into hepatocyte-like cells (HLCs) as described previously.[26]

The subgenomic HEV replicon construct harboring a neomycin phosphotransferase selection marker, a 2A self-cleaving peptide sequence, and a *Gaussia* luciferase (GLuc) reporter gene, was derived from the p6 plasmid (HEV3 Rep/GLuc2ANeo). A three-step polymerase chain reaction (PCR) using specific primers (Supporting Table S2) was performed on plasmids p6 GLuc[27] and pcDNA3.1 (Thermo Fisher Scientific, Waltham, MA), respectively, followed by overlap extension PCR, similar to our previous report.[13] In brief, HEV3 Rep/GLuc2ANeo cells were generated by transfection of *in vitro* transcribed RNA into S10-3 cells using the TransIT mRNA transfection kit (MIRUS, Madison, WI) according to the manufacturer's instructions. Three days following transfection, replicon cells were selected using 500 μg/mL G418 (Invivogen, San Diego, CA) until non-transfected control cells died.

SHRNA DESIGN AND CLONING

shRNAs against HEV GT3 Kernow-C1 p6 were designed according to the shRNA design guidelines and selection criteria provided by the InvivoGen siRNA Wizard Software (https://www.invivogen.com/sirnawizard/design.php). To minimize the risk of shRNA off-targeting activity, candidates underwent BLAST selection against the human miRNA SEED database. A 7-nt loop (Supporting Table S1) was added between the antisense and sense sequence to form shRNAs, and oligos were designed with 5′ overhangs for cloning. Forward and reverse oligos (Supporting Table S1) were annealed and cloned through Golden Gate assembly[28] using the type IIs restriction enzyme BsmBI into a self-complementary (sc)AAV plasmid backbone under a U6 promoter (as previously described in Börner et al.[29]). Cloning of the multiplexed triple shRNA plasmids was performed using a two-step Golden Gate assembly approach. First, the respective single shRNA was inserted into interim plasmids containing either the U6, H1, or 7sk promoter using BsmBI. Subsequently, the three shRNA expression cassettes were multiplexed into a self-complementary AAV (scAAV) recipient plasmid using BbsI (manuscript in preparation, in parts previously described in Pujol et al.[30] and Amoasii et al.[31]).

AAV PRODUCTION AND TITRATION

AAVs were produced and titrated as previously described,[32] and used either as crude cell lysate or purified using an iodixanol gradient. Primers and probe used for titration are listed in Supporting Table S2. AAV transductions were performed in cell culture medium without FBS, which was reverted to standard cell culture medium the next morning.

SHRNA SCREEN ON HEV REPLICON CELLS

HEV3 Rep/GLuc2ANeo cells were seeded onto 96-well plates at a density of 3×10^3 cells per well. Cells were transduced with crude lysates or purified AAV as specified in the respective figure legend the next day. Twenty-four hours later, AAVs were removed, and medium was changed to regular culture medium without G418. To measure secreted GLuc, 10 μL of culture supernatant was transferred to a white Lumitrac 200 plate (Greiner Bio-One, Frickenhausen, Germany) followed by automated injection of 100 μL reconstituted luciferase assay buffer with 1:400 diluted coelenterazine (Promega, Madison, WI). Luminescence was measured using a Glomax 96 Microplate Luminometer (Promega).

HEV PRODUCTION AND INFECTION

HEV particles based on the HEV GT3 Kernow-C1 p6 strain were produced as recently described.[13] For microscopy-based assays, 1×10^3 cells were seeded per

well in a 96-well plate and infected with HEV at a multiplicity of infection (MOI) of 0.16. Seventy-two hours later, AAV was added at a MOI of 1-5 × 10^4, as specified in the figure legends. Six days following HEV infection, cells were fixed with 4% paraformaldehyde (EMS, Hatfield, PA) and stained using an anti-ORF2 antibody (1:100, 1E6; Millipore, Burlington, MA) and a secondary anti-mouse antibody conjugated to Alexa Fluor 594 (1:1,000; Thermo Fisher), following a standard immunofluorescent staining protocol (as described in Ankavay et al.[33]). For assays requiring RNA extraction, 1 × 10^4 cells were seeded per well in a 24-well plate and infected with HEV at a MOI of 0.1. To quantify HEV genomes, RNA was extracted from HEV-infected cells at different time points as specified in the figure legends using the RNeasy Mini Kit (Qiagen, Hilden, Germany) and reverse-transcribed using the iScript cDNA Synthesis Kit (Bio-Rad, Hercules, CA). HEV positive-strand RNA and RPS11 expression were quantified with specific primers (Supporting Table S2) using iTaq Universal SYBR Green Supermix (Bio-Rad).

AUTOMATED MICROSCOPY AND KNIME ANALYSIS

For microscopy analysis, images in multiple channels (Hoechst, green fluorescent protein [GFP], Cy3) were taken in nine subpositions within each well with a 10× objective using Scan^R acquisition software (Olympus Biosystems, Shinjuku, Japan) on an automated epifluorescence microscope (Olympus Biosystems). A KNIME workflow was compiled to process the images and retrieve quantitative information (https://hub.knime.com/manuel/spaces/Public/latest/IdentifyNuclei_measure2Channels). It consists of a filename parser, which extracts image specific metadata such as well ID, well subposition, and channel information from the file name. Images were processed consecutively in a loop. First, image backgrounds were corrected by a rolling ball algorithm. Each image of the nuclear stain was thresholded (combination of Huang and manual thresholding in order to set a minimum intensity threshold[34]) and a connected component analysis was performed following the resulting binary masks, followed by cell clump splitting.[35] Based on a secondary staining in the cytoplasm, a Voronoi-based extension of the identified nuclear regions was performed to identify the regions of individual cells. For each cell, intensities of all color channels were measured within these regions. Based on these intensities, cells were classified as positive or negative in the respective color channel. AAV transduction efficiency was assessed by measuring the percentage of GFP-positive cells. For HEV infection analysis, mean fluorescence intensity of Cy3 positively stained cells as well as the percentage of positively stained cells was taken into account.

Results

SCREENING SHRNA CANDIDATES WITH HEV3 REP/GLUC2ANEO CELLS

We designed shRNAs targeting the HEV GT3 Kernow-C1 p6 genome, including noncoding and coding regions (Fig. 1A), with the exception of the hypervariable region. We excluded candidates with sequences known to induce an immune response or to have off-targets in the human genome,[36-38] yielding a panel of 20 shRNAs (Supporting Table S1). We inserted the shRNA candidates into a scAAV plasmid backbone under a U6 promoter together with a second expression cassette harboring a *gfp* reporter gene.

To screen the 20 shRNA candidates, we used HEV3 Rep/GLuc2ANeo cells. These cells were generated by transfection of S10-3 cells (an Huh-7 subclone) with a selectable reporter replicon, in which part of the genome encoding ORF2 and 3 was replaced by a *GLuc* reporter gene, followed by a 2A self-cleaving peptide as well as a neomycin resistance gene. Following selection with G418, HEV3 Rep/GLuc2ANeo cells were established in which viral replication leads to the expression and secretion of GLuc. GLuc levels could then be conveniently measured in the cellular supernatant to serve as a quantitative reporter for HEV replication.

We performed an AAV capsid screen on S10-3 cells to maximize shRNA delivery efficiency and identified AAV6 as the capsid variant with the highest transduction efficiency (Supporting Fig. S1). We then packaged the shRNA candidates in AAV6 capsids and transduced HEV3 Rep/GLuc2ANeo cells. Comparable GFP expression levels of about 90% confirmed similar transduction rates and thus implied similar shRNA expression efficiencies among

the different AAV6-shRNA vectors. We measured secreted GLuc in the supernatant 72 hours following transduction to assess the effect of the shRNA candidates on HEV replication. As shown in Fig. 1B, the shRNAs inhibited GLuc secretion with varying potencies. For example, while shRNA 18 had no effect compared with mock-treated cells, shRNA 20 reduced secreted GLuc levels by up to 98%. Of note, the inhibitory effect of several shRNA candidates exceeded the potency of daily RBV applications, which we included as positive control. Importantly, we performed cell viability assays to rule out unspecific effects of AAV6-shRNA transduction (Fig. 1B).

Based on this first screen, we selected the top five inhibitory shRNAs (i.e., shRNAs 2, 3, 8, 19, and 20). In a second screen using purified and titrated AAVs, we identified shRNAs 2, 8, and 20 as the three most potent shRNAs to inhibit HEV replication (Supporting Fig. S2). They target the methyltransferase (shMet), the base of an intrinsic stem-loop in ORF 2 (shISLB, previously described as being crucial for HEV replication[39]), and the 3´ end of ORF 2 (shORF2), respectively.

INHIBITION OF FULL-LENGTH HEV GT3 INFECTION WITH SELECTED SHRNA CANDIDATES

We then sought to test the capacity of the three most potent shRNAs to also inhibit full-length HEV replication. To this end, we infected S10-3 cells with the HEV GT3 Kernow-C1 p6 virus. Seventy-two hours following infection, we transduced the cells with the three AAV6-shRNAs (Fig. 2). As a nontargeting control, we used an shRNA designed against the hepatitis D virus genome (shCtrl). Twenty-four hours following transduction, we removed the AAVs, and HEV infection was allowed to continue for additional 48 hours.

We first assessed the effect of the AAV6-shRNAs on HEV replication by HEV ORF2 capsid staining of infected cells (Fig. 2A). Compared with mock-transduced and AAV6-shCtrl-transduced cells, we observed a substantial decrease of ORF2 expression in cells transduced with shMet, shISLB, and shORF2. The overall quantification of ORF2 staining (based on number of positively stained cells as well as fluorescence intensity per cell) revealed that shRNAs directed against the HEV genome reduced ORF2 expression by up to 50%. AAV6-shORF2 was the most potent construct with a reduction of up to 60% (Fig. 2B). As shown in Fig. 2A, HEV infection events preferentially took place in cells that were not transduced with AAV6, as evidenced by the absence of GFP expression in ORF2-positive cells.

We also measured the effect of AAV6-shRNA transduction on viral genome copy numbers as quantified by quantitative real-time PCR over a prolonged time of HEV infection (up to 21 days) (Fig. 2C). Cells transduced with AAV6-shCtrl replicated to similar levels as mock-transduced cells. In contrast, in cells transduced with AAV-shMet, shISLB, or shORF2, HEV replication was decreased by up to two logs. In cells transduced with AAV6-shMet and AAV6-shORF2, HEV replication remained low, whereas viral genome copy numbers slowly increased over time in cells transduced with AAV6-shISLB.

MULTIPLEXING ANTI-HEV SHRNAS FOR A SUSTAINED LONG-TERM INHIBITORY EFFECT

To enable long-term HEV inhibition and prevent resistance escape mutations, we multiplexed the three shRNAs for co-expression from a single AAV vector (Fig. 3A), in which all three shRNAs were cloned under different promoters, namely U6, 7sk, and H1. As a control, the sequences of the three shRNAs were scrambled and multiplexed as a triple scrambled control (trish scrbl Ctrl). In addition, we also multiplexed each of the functional shRNAs with two scrambled sequences for comparison with the single shRNA.

Similar to our results with the single shRNAs, HEV ORF2 staining was notably decreased in HEV-infected cells transduced with the multiplexed shRNA construct (Fig. 3B). Compared with the single shRNA constructs, which decreased ORF2 expression by up to 50% (Figs. 2C and 3B), transduction with the multiplexed shRNA construct decreased ORF2 expression up to 80%. As expected, we found that multiplexing two scrambled shRNAs with each of the functional anti-HEV shRNAs showed no significant improvement of inhibition compared with the single shRNA construct alone. Moreover, neither the AAV6-shCtrl nor the AAV6-trish scrbl control appreciably inhibited HEV ORF2 expression.

We also investigated the effect on HEV-RNA levels over a prolonged period of up to 21 days (Fig. 3C). Compared with the AAV6-trish scrbl control, which

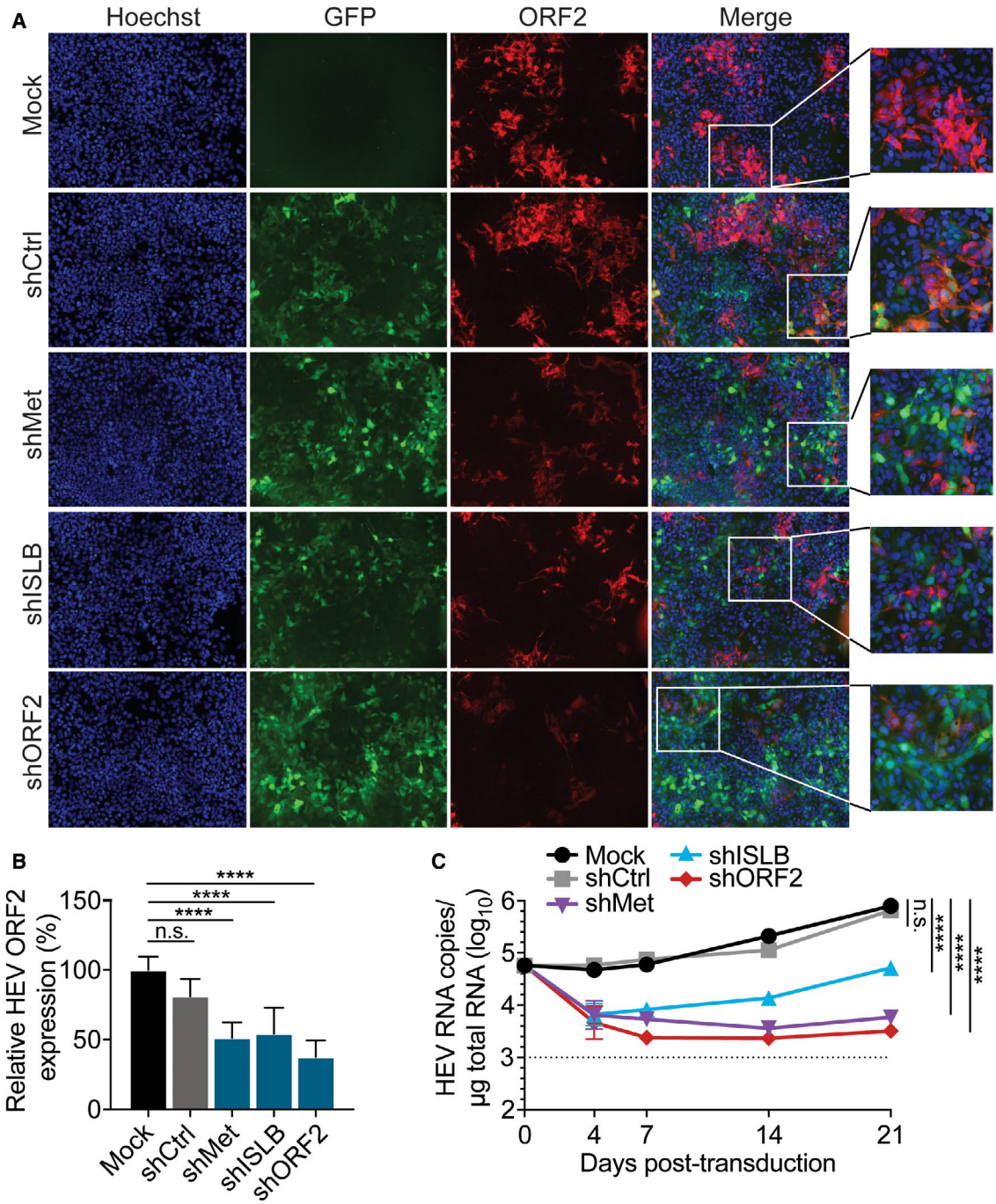

FIG. 2. AAV6-mediated shRNA delivery down-regulates HEV capsid ORF2 expression and viral genomes in HEV-infected cells. Immunofluorescence staining (A) and quantification (B) of ORF2 expression in HEV GT3 Kernow-C1 p6 virus-infected S10-3 cells (HEV MOI 0.16) transduced with AAV6-shRNAs (AAV MOI 10^4) 72 hours following infection with HEV. Seventy-two hours following transduction, cells were fixed and stained with an ORF2 antibody (red) and Hoechst (blue). AAV6-transduced cells are GFP-positive (green). (B) Relative ORF2 expression was calculated based on the mean fluorescence intensity (MFI) and percentage of ORF2 positively stained cells normalized to mock-transduced cells. Results represent the mean of n = 6 ± SD. (C) HEV genome copies of infected S10-3 cells (HEV MOI 0.1) transduced 72 hours following infection with specified AAV6-shRNA constructs (MOI 5×10^4), quantified by quantitative real-time PCR analysis at indicated time points following AAV6 transduction. The dotted line indicates the limit of quantification. Results represent the mean of n = 3 ± SEM. Statistical analysis was performed using a one-way analysis of variance (ANOVA) followed by Tukey's *post hoc* test. ****$P < 0.0001$. Abbreviations: n.s., not significant; and shCtrl, control shRNA.

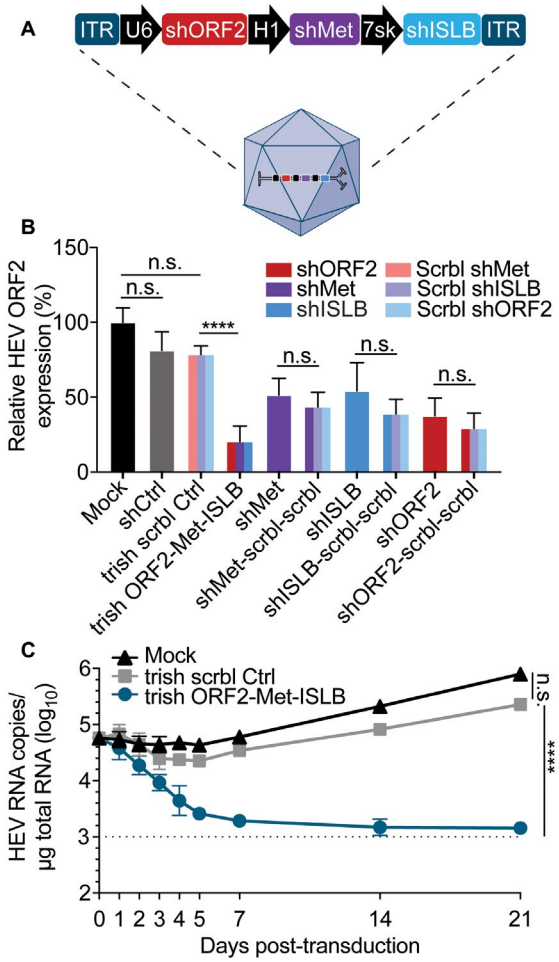

FIG. 3. Multiplexing shRNAs leads to long-term inhibitory effect on HEV replication. (A) Schematic depiction of the multiplexed AAV vector. The three most potent shRNAs or their respective scrambled counterparts were multiplexed under three different promoters (U6, 7sk, and H1). The transgene is flanked by two inverted terminal repeats (ITRs) necessary for packaging into AAVs. (B) Quantification of ORF2 expression in HEV-infected S10-3 cells (HEV MOI 0.16) transduced with AAV6-shRNA vectors (MOI = 10^4) as indicated. Cells were fixed 72 hours following transduction, and HEV ORF2 staining was assessed via automated microscopy analysis. Dark colors represent target shRNAs and light colors their respective scrambled controls. Note that the fourth, sixth, and eighth construct each contain one targeted and two scrambled shRNAs. Results represent the mean of n = 6 ± SD. (C) HEV genome copies in infected S10-3 cells (HEV MOI 0.1) transduced with the indicated shRNA-encoding AAV (MOI = 5×10^4), quantified by quantitative real-time PCR analysis at indicated time points following AAV6 transduction. The dotted line indicates the limit of quantification. Results represent the mean of n = 3 ± SEM. Statistical analysis was performed using one-way ANOVA followed by Tukey's *post hoc* multiple comparisons test. ****$P < 0.0001$. Abbreviations: trish scrbl Ctrl, multiplexed triple scrambled shRNA control; and trishMet-ISLB-ORF2, multiplexed triple shRNAs targeting Met, ISLB, and ORF2.

did not significantly suppress HEV replication, the AAV6-multiplexed shRNAs decreased HEV replication to almost undetectable levels by day 21 following transduction. This was accompanied by a substantial viral protein loss over the observation period in the multiplexed AAV6-shRNA sample, but not in the controls, as detected by ORF2 staining (Supporting Fig. S3).

VALIDATION OF SHRNAS IN HEV-INFECTED INDUCED PLURIPOTENT-DERIVED HEPATOCYTE-LIKE CELLS

Finally, we aimed to confirm the inhibitory potency of our shRNA candidates using iPSC-derived HLCs, which are more suitable to study HEV biology than hepatoma cells.[26] We first screened different AAV capsid variants for their transduction efficiency on HLCs (Supporting Fig. S4). Similar to our results on S10-3 cells, we identified AAV6 as the most efficient capsid variant.

We then infected HLCs with HEV and transduced them with AAV6-shRNAs 72 hours following infection (Fig. 4). After additional 72 hours, we measured HEV replication by quantifying HEV genomes through quantitative real-time PCR. HEV replication was decreased by up to 66% with the single shRNAs (Fig. 4A) and even further with the multiplexed shRNA (Fig. 4B). In contrast, the AAV6-shCtrl or AAV6-trish scrbl control did not significantly decrease HEV replication. These results confirmed the anti-HEV inhibitory potency of the identified shRNAs in a physiologically relevant culture system.

Discussion

Specific anti-HEV treatments are needed, especially for chronic patients who fail current treatment options or who cannot tolerate them.[11] In the present study, we screened and identified shRNAs that efficiently downregulated replication of HEV GT3, the leading genotype responsible for chronic infections. In extension to the previous study on HEV GT1,[22] we also validated the inhibitory potency of shRNAs on full-length HEV infection. Moreover, we confirmed their potency in iPSC-derived HLCs, which are more physiologically relevant than hepatoma cells.[26] Furthermore,

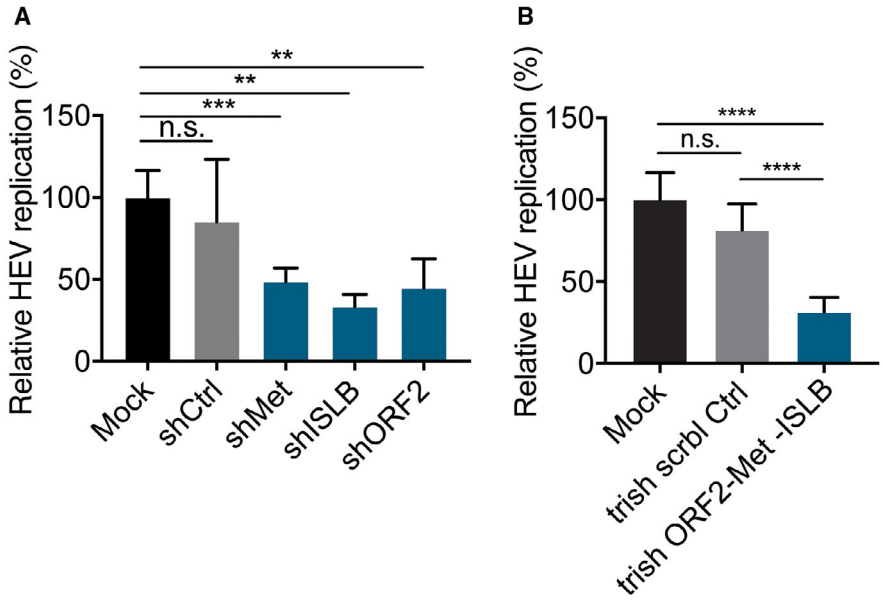

FIG. 4. AAV6-delivered shRNAs down-regulate HEV replication in hepatocyte-like cells. HEV genomes in infected (HEV MOI = 0.1) induced pluripotent stem cell–derived HLCs 7 days following transduction with AAV6 (MOI = 5×10^4) constructs encoding single (A) or multiplexed shRNAs (B) quantified by quantitative real-time PCR. Replication levels were normalized to an untreated mock control. Results represent the mean of n = 6 ± SD. Statistical analysis was performed using one-way ANOVA followed by Tukey's *post hoc* multiple comparisons test. $^{**}P < 0.01$; $^{***}P < 0.001$; $^{****}P < 0.0001$.

our approach is curative and not preventive, as compared with a study in which shRNAs conferred protection against subsequent HEV GT4 infection.[27] The proposed combination with AAV delivery, which has been established as a promising and safe vehicle for *in vivo* transduction including in humans, underlines its potential for clinical application.[24,25]

Using an established subgenomic reporter replicon based on the HEV GT3 Kernow-C1 strain, we identified three suitable RNAi target regions. These regions include areas encoding the methyltransferase, ORF2, and the base of a highly conserved intrinsic stem-loop essential for replication described by Emerson et al.[39] The combination of the accessibility of these target sequences for the shRNA together with their importance and/or conservation for HEV replication likely explains the robust effects observed here.

Previous work with RNAi has raised concerns regarding the overexpression of shRNA, which may lead to oversaturation of the endogenous miRNA pathway and therefore trigger adverse cytotoxicity.[40] Adjusting shRNA expression levels by optimizing vector dosage or by using tissue-specific promoters circumvented this problem.[40,41] Therefore, identifying the most potent shRNAs was of paramount importance in this work, as it should allow us to lower vector dosages. In our multiplexed approach, we used three different RNA polymerase III promoters, which enabled fine-tuning of shRNA expression levels. When designing the original shRNA panel, we also considered other potential toxicity concerns by excluding sequences known to induce immune responses.[36-38] As a result, none of the shRNAs induced cytotoxicity at the tested AAV vector dosages (Fig. 1B).

We noted that targeting the *Met* gene and the 3′ end of ORF2 mediated a sustained inhibitory effect, whereas the reduction in HEV genome replication waned about 1 week following transduction with shRNA ISLB. Although the dissection of the exact mechanism(s) underlying the latter was beyond the focus of this work, one possible explanation is the slightly lower efficiency of this particular shRNA as compared with the other two shRNAs (Fig. 2). This could have enabled HEV to replicate more effectively and more quickly in the presence of this shRNA, as opposed to the more potent shRNAs shMet and shORF2. In line with this, we found that the shRNA that yielded the strongest HEV

ORF2 knockdown, shORF2 (Fig. 2B), also mediated the most persistent HEV-RNA inhibition over time (Fig. 2C). Alternatively, or in addition, we note a challenge that has become apparent when applying RNAi-based strategies to other viruses, which is the rapid emergence of viral escape mutants.[21] This has often been reported after treatment with a single siRNA, whereas combining two siRNAs targeting different areas was sufficient to prevent this adverse event.[19] To proactively counter this concern, we harnessed an original AAV vector design from our lab,[35] which allowed us to multiplex the three most efficient shRNAs under different promoters in a single AAV backbone. Compared with the targeting of a single region in HEV, transduction with the triple shRNA construct led to stronger and, more importantly, sustained HEV replication inhibition, reducing HEV genome levels close to the detection limit over the observed time (21 days) (Fig. 3). Regardless of the putative mechanism(s) explaining the differences between the individual shRNAs, this result showcases the benefits of shRNA multiplexing in a single AAV vector over their separate expression, in line with, and extending, previous findings from our group.[30]

Because HEV primarily replicates in hepatocytes, we identified a suitable AAV capsid variant, AAV6, to efficiently transduce both the hepatoma cell line S10-3 and iPSC-derived HLCs *in vitro*. We are aware that this AAV serotype may not be the best choice for *in vivo* transduction, as substantial discrepancies in transduction efficiency between *in vivo* and *in vitro* as well as between species have been reported.[42] For clinical translation in patients infected with HEV patients, it should therefore be beneficial to pseudotype the shRNA permutations from our study with a better-suited AAV capsid selected from the available and extensive assortment of naturally occurring or molecularly evolved synthetic capsids.

In chronic patients, extrahepatic HEV manifestations and detection of HEV RNA in cerebrospinal fluid,[43] kidney cryoprecipitate,[44] intestine,[45] and more, were reported. These observations hint at additional cellular targets for the proposed RNAi treatment. AAV capsids can be engineered as tissue-specific delivery vehicles, and the combination with tissue-specific promoters will enable targeting these extrahepatic HEV reservoirs in the future.

Considering the widely documented safety of AAV vector-based gene therapies (reviewed in Borel et al.[24] and Zhan et al.[25]) as well as the recent FDA approval of AAV vector-based therapies for retinal dystrophy (Luxturna)[46] or spinal muscular atrophy (Zolgensma),[47] our proof-of-concept study to combine AAV and multiplexed shRNAs is, in principle, amenable to clinical translation. Ultimately, it could be used as an alternative treatment method for patients with chronic HEV who do not respond well to established therapies.

Acknowledgment: The authors thank Suzanne U. Emerson for sharing reagents.

REFERENCES

1) Kamar N, Izopet J, Pavio N, Aggarwal R, Labrique A, Wedemeyer H, et al. Hepatitis E virus infection. Nat Rev Dis Primers 2017;3:17086.
2) Oechslin N, Moradpour D, Gouttenoire J. On the host side of the hepatitis E virus life cycle. Cells 2020;9:1294.
3) Kinast V, Burkard TL, Todt D, Steinmann E, Hepatitis E virus drug development. Viruses. 2019;11.
4) van Tong H, Hoan NX, Wang B, Wedemeyer H, Bock CT, Velavan TP. Hepatitis E virus mutations: functional and clinical relevance. EBioMedicine 2016;11:31-42.
5) Purdy MA, Harrison TJ, Jameel S, Meng XJ, Okamoto H, Van der Poel WHM, et al. ICTV virus taxonomy profile: hepeviridae. J Gen Virol 2017;98:2645-2646.
6) Mullhaupt B, Niederhauser C. Hepatitis E blood donor screening—more than a mere drop in the ocean? J Hepatol 2018;69:8-10.
7) Lee GH, Tan BH, Teo EC, Lim SG, Dan YY, Wee A, et al. Chronic infection with camelid hepatitis E virus in a liver transplant recipient who regularly consumes camel meat and milk. Gastroenterology 2016;150:e353.
8) Sridhar S, Yip C-Y, Wu S, Chew N-S, Leung K-H, Chan J-W, et al. Transmission of rat hepatitis E virus infection to humans in Hong Kong: a clinical and epidemiological analysis. Hepatology 2020;73:10-22.
9) Pérez-Gracia MT, Suay-García B, Mateos-Lindemann ML. Hepatitis E and pregnancy: current state. Rev Med Virol 2017;27:e1929.
10) Horvatits T, Pischke S. Extrahepatic manifestations and HEV, the genotype matters. EBioMedicine 2018;36:3-4.
11) European Association for the Study of the Liver. EASL Clinical Practice Guidelines on hepatitis E virus infection. J Hepatol 2018;68:1256-1271.
12) **Debing Y**, **Gisa A**, Dallmeier K, Pischke S, Bremer B, Manns M, et al. A mutation in the hepatitis E virus RNA polymerase promotes its replication and associates with ribavirin treatment failure in organ transplant recipients. Gastroenterology 2014;147:1008-1011.e1007; quiz e1015-e1006.
13) Dao Thi VL, Debing Y, Wu X, Rice CM, Neyts J, Moradpour D, et al. Sofosbuvir inhibits hepatitis E virus replication in vitro and results in an additive effect when combined with ribavirin. Gastroenterology 2016;150:e84.
14) Cornberg M, Pischke S, Müller T, Behrendt P, Piecha F, Benckert J, et al. Sofosbuvir monotherapy fails to achieve HEV RNA elimination in patients with chronic hepatitis E—the HepNet SofE pilot study. J Hepatol 2020;73:696-699.
15) Schuster S, Miesen P, van Rij RP. Antiviral RNAi in insects and mammals: parallels and differences. Viruses 2019;11:448.
16) Bobbin ML, Rossi JJ. RNA Interference (RNAi)-based therapeutics: delivering on the promise? Annu Rev Pharmacol Toxicol 2016;56:103-122.

17) Second RNAi drug approved. Nat Biotechnol 2020;38:385.
18) Scott LJ, Keam SJ. Lumasiran: first approval. Drugs 2021;81: 277-282.
19) ter Brake O, Konstantinova P, Ceylan M, Berkhout B. Silencing of HIV-1 with RNA interference: a multiple shRNA approach. Mol Ther 2006;14:883-892.
20) Michler T, Grosse S, Mockenhaupt S, Roder N, Stuckler F, Knapp B, et al. Blocking sense-strand activity improves potency, safety and specificity of anti-hepatitis B virus short hairpin RNA. EMBO Mol Med 2016;8:1082-1098.
21) Kronke J, Kittler R, Buchholz F, Windisch MP, Pietschmann T, Bartenschlager R, et al. Alternative approaches for efficient inhibition of hepatitis C virus RNA replication by small interfering RNAs. J Virol 2004;78:3436-3446.
22) Kumar A, Panda SK, Durgapal H, Acharya SK, Rehman S, Kar UK. Inhibition of hepatitis E virus replication using short hairpin RNA (shRNA). Antiviral Res 2010;85:541-550.
23) Huang F, Hua X, Yang S, Yuan C, Zhang W. Effective inhibition of hepatitis E virus replication in A549 cells and piglets by RNA interference (RNAi) targeting RNA-dependent RNA polymerase. Antiviral Res 2009;83:274-281.
24) Borel F, Kay MA, Mueller C. Recombinant AAV as a platform for translating the therapeutic potential of RNA interference. Mol Ther 2014;22:692-701.
25) **Zhan W**, **Muhuri M**, Tai PWL, Gao G. Vectored immunotherapeutics for infectious diseases: can rAAVs be the game changers for fighting transmissible pathogens? Front Immunol 2021;12:673699.
26) **Wu X**, **Dao Thi VL**, Liu P, Takacs CN, Xiang K, Andrus L, et al. Pan-genotype hepatitis E virus replication in stem cell-derived hepatocellular systems. Gastroenterology 2018;154:e667.
27) Shukla P, Nguyen HT, Faulk K, Mather K, Torian U, Engle RE, et al. Adaptation of a genotype 3 hepatitis E virus to efficient growth in cell culture depends on an inserted human gene segment acquired by recombination. J Virol 2012;86:5697-5707.
28) Engler C, Kandzia R, Marillonnet S. A one pot, one step, precision cloning method with high throughput capability. PLoS One 2008;3:e3647.
29) Börner K, Niopek D, Cotugno G, Kaldenbach M, Pankert T, Willemsen J, et al. Robust RNAi enhancement via human Argonaute-2 overexpression from plasmids, viral vectors and cell lines. Nucleic Acids Res 2013;41:e199.
30) Pujol FM, Laketa V, Schmidt F, Mukenhirn M, Müller B, Boulant S, et al. HIV-1 Vpu antagonizes CD317/tetherin by adaptor protein-1-mediated exclusion from virus assembly sites. J Virol 2016;90:6709-6723.
31) **Amoasii L**, **Long C**, Li H, Mireault AA, Shelton JM, Sanchez-Ortiz E, McAnally JR, et al. Single-cut genome editing restores dystrophin expression in a new mouse model of muscular dystrophy. Sci Transl Med 2017;9:eaan8081.
32) Fakhiri J, Nickl M, Grimm D. Rapid and simple screening of CRISPR guide RNAs (gRNAs) in cultured cells using adeno-associated viral (AAV) vectors. Methods Mol Biol 2019;1961: 111-126.
33) Ankavay M, Montpellier C, Sayed IM, Saliou J-M, Wychowski C, Saas L, et al. New insights into the ORF2 capsid protein, a key player of the hepatitis E virus lifecycle. Sci Rep 2019;9:6243.
34) Pujol FM, Laketa V, Schmidt F, Mukenhirn M, Muller B, Boulant S, et al. HIV-1 Vpu antagonizes CD317/Tetherin by adaptor protein-1-mediated exclusion from virus assembly sites. J Virol 2016;90:6709–6723.
35) Wahlby C, Sintorn IM, Erlandsson F, Borgefors G, Bengtsson E. Combining intensity, edge and shape information for 2D and 3D segmentation of cell nuclei in tissue sections. J Microsc 2004;215:67-76.
36) Hornung V, Guenthner-Biller M, Bourquin C, Ablasser A, Schlee M, Uematsu S, et al. Sequence-specific potent induction of IFN-alpha by short interfering RNA in plasmacytoid dendritic cells through TLR7. Nat Med 2005;11:263-270.
37) Judge AD, Sood V, Shaw JR, Fang D, McClintock K, MacLachlan I. Sequence-dependent stimulation of the mammalian innate immune response by synthetic siRNA. Nat Biotechnol 2005;23:457-462.
38) Lan T, Putta MR, Wang D, Dai M, Yu D, Kandimalla ER, et al. Synthetic oligoribonucleotides-containing secondary structures act as agonists of Toll-like receptors 7 and 8. Biochem Biophys Res Commun 2009;386:443-448.
39) Emerson SU, Nguyen HT, Torian U, Mather K, Firth AE. An essential RNA element resides in a central region of hepatitis E virus ORF2. J Gen Virol 2013;94:1468-1476.
40) Grimm D, Streetz KL, Jopling CL, Storm TA, Pandey K, Davis CR, et al. Fatality in mice due to oversaturation of cellular microRNA/short hairpin RNA pathways. Nature 2006;441: 537-541.
41) Sun CP, Wu TH, Chen CC, Wu PY, Shih YM, Tsuneyama K, et al. Studies of efficacy and liver toxicity related to adeno-associated virus-mediated RNA interference. Hum Gene Ther 2013;24:739-750.
42) Kay MA. Selecting the best AAV capsid for human studies. Mol Ther 2015;23:1800-1801.
43) Fritz M, Berger B, Schemmerer M, Endres D, Wenzel JJ, Stich O, et al. Pathological cerebrospinal fluid findings in patients with neuralgic amyotrophy and acute hepatitis e virus infection. J Infect Dis 2018;217:1897-1901.
44) Guinault D, Ribes D, Delas A, Milongo D, Abravanel F, Puissant-Lubrano B, et al. Hepatitis E virus-induced cryoglobulinemic glomerulonephritis in a nonimmunocompromised person. Am J Kidney Dis 2016;67:660-663.
45) Marion O, Lhomme S, Nayrac M, Dubois M, Pucelle M, Requena M, et al. Hepatitis E virus replication in human intestinal cells. Gut 2020;69:901-910.
46) FDA. FDA approves novel gene therapy to treat patients with a rare form of inherited vision loss. FDA Press Announcements; 2017.
47) Keeler AM, Flotte TR. Recombinant adeno-associated virus gene therapy in light of Luxturna (and Zolgensma and Glybera): where are we, and how did we get here? Annu Rev Virol 2019;6:601-621.

Author names in bold designate shared co-first authorship.

Supporting Information

Additional Supporting Information may be found at onlinelibrary.wiley.com/doi/10.1002/hep4.1842/suppinfo.